Available online at www.sciencedirect.com
ScienceDirect
Journal of Power Sources 164 (2007) 322–327
JOURNAL OF POWER SOURCES
www.elsevier.com/locate/jpowsour

Short communication

Power characteristics and fluid transfer in 40 W direct methanol fuel cell stack

Yang Liu [a], Xiaofeng Xie [a,*], Yuming Shang [a], Rong Li [a], Liang Qi [a], Jianwei Guo [a], V.K. Mathur [b]

[a] *Institute of Nuclear and New Energy Technology, Tsinghua University, Beijing 100084, China*
[b] *Department of Chemical Engineering, University of New Hampshire, New Hampshire 03824, USA*

Received 14 June 2006; received in revised form 5 August 2006; accepted 15 September 2006
Available online 28 November 2006

Abstract

The methanol crossover, water transfer and power characteristics of a 40 W DMFC stack are investigated under various experimental conditions including different methanol concentrations, flow rates at anode and cathode and flow directions of reactant fluids (methanol solution and air). The performance of each cell in a stack shows some non-uniformity especially at higher current densities. Under Z-type flow direction the cells exhibit more uniform behavior than when under U-type flow. The performance of a stack supplied with 1 M methanol solution is much better than with 0.5 M solution. However, an increased amount of methanol crossover and water transfer across the membrane have been observed. The reactants flow rates at the anode and cathode are found to affect the fluid transfer and cell performance. At a feed of 1 M methanol solution and ambient air pressure the maximum power output of the stack is estimated to be about 50 W (90 mW cm^{-2}). The maximum power density in a stack is about 87% of that of the optimum single cell power before being assembled into a stack.

Keywords: DMFC; Fuel stack; Power characteristics; Methanol crossover; Water transfer

1. Introduction

Direct methanol fuel cell (DMFC) is regarded a promising source for portable power of high power density as well as a convenient power storage device [1–3]. However, there are still some technological obstacles, such as low electro-activity of methanol oxidation at the anode and methanol crossover through the membrane, hindering their commercialization. Anode electronic kinetics limits the power characteristics. Methanol crossover produces mixed potential at the cathode reducing the cell efficiency.

Most single cell research work has been conducted on new materials for electrolyte membranes and catalysts for anode and cathode [4–7] to improve cell power characteristics. As for a DMFC stack, studies include designing appropriate stack structure and optimizing experimental operating conditions [8–15] particularly with regard to methanol crossover and water management at the cathode.

In this investigation, after obtaining the optimum operating conditions for a single cell, a 40 W DMFC stack comprising of 20 cells has been assembled to investigate the methanol crossover, water transfer across the membrane and power characteristics under various operating conditions. The best stack performance is obtained using 1 M methanol solution, air at room temperature and ambient pressure and flow rates of 31 g min^{-1} and 6 slm, respectively. The maximum power achieved is about 50 W (90 mW cm^{-2}) at 7 A (250 mA cm^{-2}).

Considering the limitations of stability and life of a cell stack, we selected 5 A as the rated current and the corresponding rated power of 40 W. The stack temperature is maintained at 50 °C. Stoichiometric methanol and air flow rates are 3 (31.49 g min^{-1}) and 3.62 (6 slm), respectively. The Faraday efficiency as calculated by Eq. (1) is 83.3%:

$$\eta = \frac{N_{\mathrm{MeOH},4}}{N_{\mathrm{MeOH},4} + N_{\mathrm{MeOH},3}} \times 100\% = 83.3\% \quad (1)$$

where $N_{\mathrm{MeOH},4}$ = mols oxidized; $N_{\mathrm{MeOH},3}$ = mols crossover.

* Corresponding author. Tel.: +86 10 62784827; fax: +86 10 62771150.
E-mail address: xiexf@mail.tsinghua.edu.cn (X. Xie).

0378-7753/$ – see front matter © 2006 Elsevier B.V. All rights reserved.
doi:10.1016/j.jpowsour.2006.09.017

2. Experimental procedure

The membrane electrode assembly (MEA) consists of a polymer membrane, anode and cathode catalyst layers and two gas diffusion layers. Nafion115 (Dupont®) is used as a membrane. By using a CCM (catalyst coated membrane) technique, the anode and cathode catalysts are coated on the either side of the membrane directly. The catalysts used for anode and cathode are PtRu black (50:50%, Johnson Matthey) and 60% Pt/C (Johnson Matthey), respectively, and their metal loadings are 4 and 3 mg cm^{-2}. A hydrophobic carbon paper (Toray-90) coated with a mixture of PTFE and carbon powder (XC-72) is used as an electrode substrate. The membrane coated with catalysts and Toray carbon paper as GDLs are used to prepare the MEA. The flow patterns (channels) in the bipolar plates are carefully machined to obtain the best performance for a single cell. Similar flow patterns are then used for cells in a stack. The stack consists of 20 cells with an active area of 27.5 cm^2 each cell. There are two copper plate as current collectors and two epoxy resin end plates at the two ends of a stack as shown in Fig. 1(a). The cell pitch is 3.2 mm. The stack specifications are presented in Table 1.

Table 1
Stack specifications

Stack	
No. of cells	20
Electrode area	27.5 cm^2
Cell pitch	3.2 mm
Size	76 mm × 103 mm × 89 mm
Maximum performance	50 W, 90 mW cm^{-2} (55 °C, ambient air pressure)
Design data	
Current	5 A
Voltage	8 V
Power density	70 mW cm^{-2}
MEA	
Membrane	Nafion115
Anode	4 mg PtRu cm^{-2}
Cathode	3 mg Pt cm^{-2}

The test system consists of the stack, an electronic load (ITECH IT8512C), a methanol solution tank, a heat exchanger

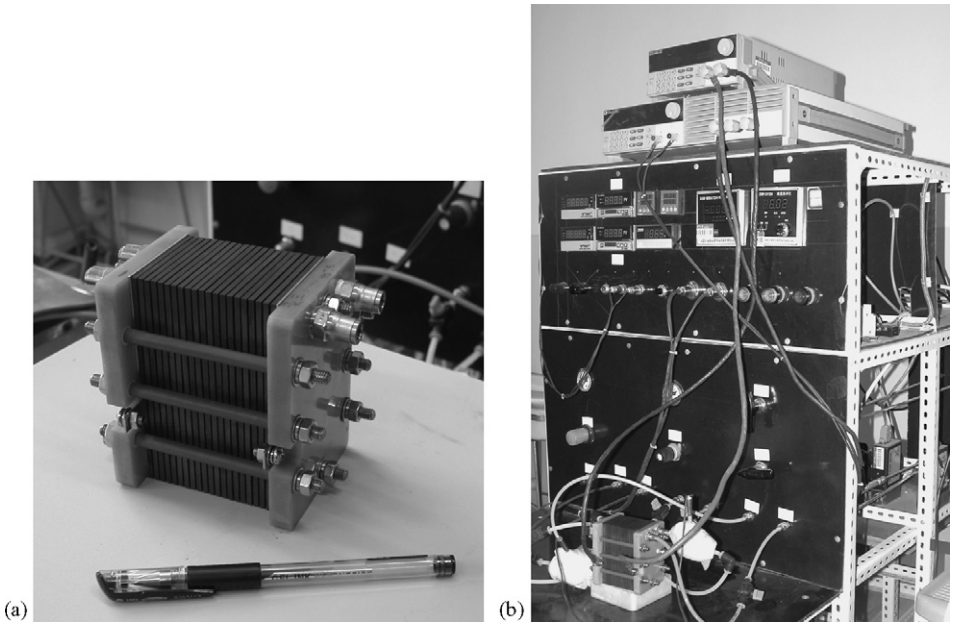

Fig. 1. Photograph of 40 W DMFC stack (a) and testing system (b).

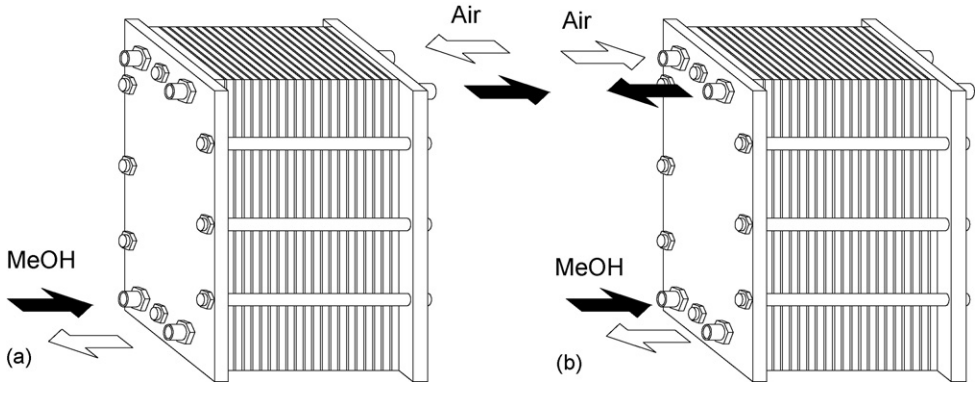

Fig. 2. Flow directions of Z-type (a) and U-type (b) in cell stack.

up stream of the stack, a cooler after the stack, a gear pump (Micro Pump 120) for pumping methanol solution and an air compressors as shown in Fig. 1(b). All experimental data are taken at cell temperatures in the range of 50–55 °C and ambient pressure. The Z- and U-type flow patterns [16] as shown in Fig. 2 are investigated by passing reactants through the stack. Details can be found elsewhere [17].

3. Mass transfer in stack

Mass transfer in a stack mainly includes methanol crossover and water transfer across the membrane. Many studies have reported on the methanol crossover in a single cell using CO_2 analysis at the cathode and anode [8,10,15,17–21]. For a power stack exceeding 10 W, this method of estimating methanol crossover may not be suitable because of excessive CO_2 production. It is observed that methanol crossover data for a single cell cannot be directly used for cells in a stack since flow and temperature distribution for cells in a stack are not uniform. The present study estimates both the methanol crossover and water transfer with flux difference and coulomb integral as discussed later.

Fig. 3 shows reactions and mass transfer in a DMFC. Methanol entering into a cell ($N_{MeOH,1}$) is divided into three parts: one part ($N_{MeOH,4}$) is oxidized at anode catalyst layer to produce H protons, another part ($N_{MeOH,3}$) crosses over membrane and most of it is oxidized at cathode to produce CO_2 and H_2O, the remaining part ($N_{MeOH,2}$) flows out of the cell. The oxidation product of methanol at anode is regarded as only CO_2 produced at high surface area of PtRu catalyst [22,23]. $N_{MeOH,4}$ and $N_{H_2O,4}$ can be calculated with Eq. (2) at constant current:

$$N_{MeOH,4} = N_{H_2O,4} = \frac{\int_0^t I\,dt}{6tF} = \frac{I}{6F} \quad (2)$$

where I is the current, t the time and F is the Faraday constant. The methanol flux is estimated by measuring inlet and outlet solution flow rates and their methanol concentrations. Methanol concentrations are determined by a gas chromatograph (SHIMAZU GC-14B). Therefore, methanol crossover and water transfer can be calculated with Eqs. (2)–(4):

$$N_{MeOH,3} = N_{MeOH,1} - N_{MeOH,2} - N_{MeOH,4} \quad (3)$$

$$N_{H_2O,3} = N_{H_2O,1} - N_{H_2O,2} - N_{H_2O,4} \quad (4)$$

Power output:

$$W = IV \quad (5)$$

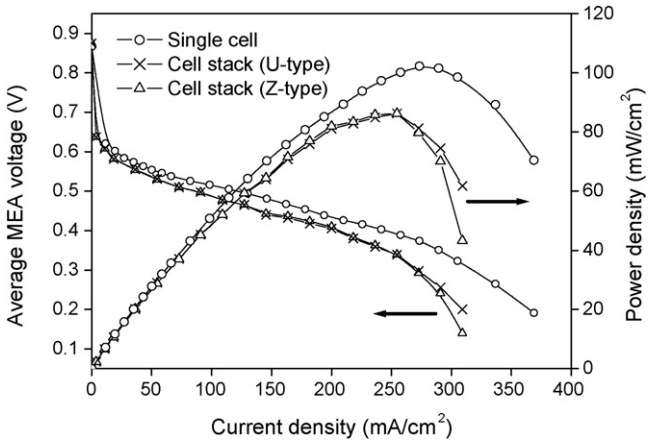

Fig. 4. Comparison of single cell and cell stack performance at 50 °C; 1 M methanol flow rate 1.6 g min^{-1}; air flow rate 300 sccm.

4. Results and discussion

4.1. Effect of different flow patterns

Fig. 4 shows average MEA performance and power characteristics of a single cell and a stack with U- and Z-type flows at 50 °C all operating under the same experimental conditions. The performance of the stack with Z- and U-type flows is found to be almost the same. The average cell power density in stack with each type of flow is about 87% of that of a single cell.

The voltage distributions over individual cells in the stack with Z- and U-type flows are shown in Fig. 5. The voltage distribution with Z-type flow is more uniform especially at the higher current of 6 A. This flow direction enhances uniformity in individual cells, thus increasing stability and life of the stack. In

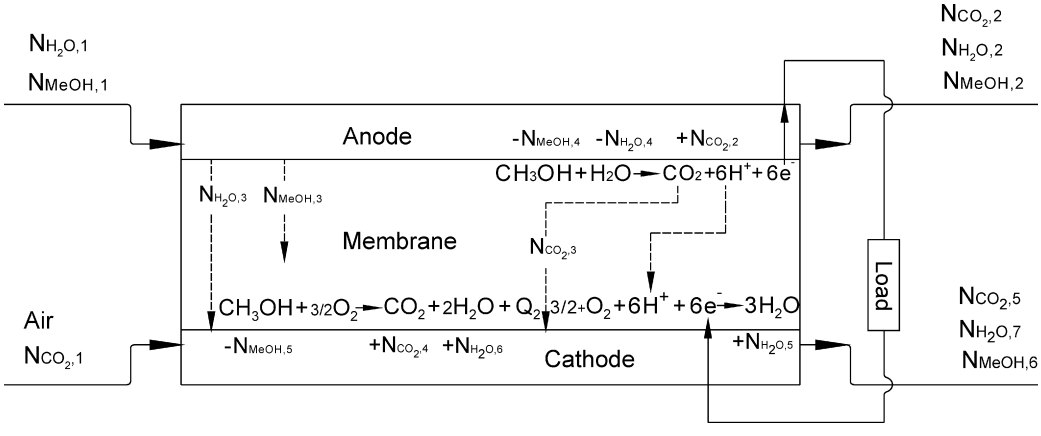

Fig. 3. Schematic diagram of reactions and mass transfer in DMFC.

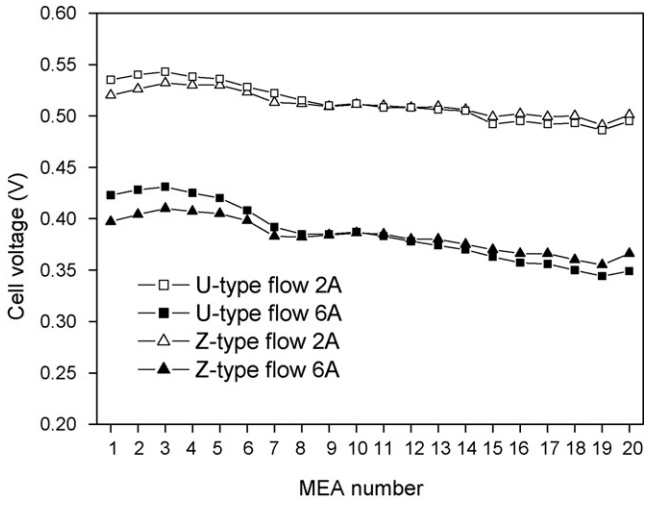

Fig. 5. Comparison of voltage distribution over individual cells in stack with U- and Z-type flow at 50 °C; 1 M methanol flow rate 31.49 g min^{-1}; air flow rate 6 slm.

the Z-type, the flow is counter current that helps in the heat and mass transfer operation which improves the efficiency. At higher methanol and air rates there is more turbulence in the channels causing more methanol crossover. The non-uniformity in voltage distribution is caused because the temperature at every cell, liquid and gas flow through each channel of each cell (of the stack) are not the same and constant. At higher current densities the reactant flow amounts are greater creating added turbulence and fluctuations. All these lead to greater non-uniformity. However, the U-type flow design can reduce the volume of stack and pipeline in the system. In this study, a Z-type flow is chosen to investigate the effect of various operating parameters.

As shown in Fig. 6, with Z-type flow the non-uniformity in voltage distribution increases with current density. When current is increased higher than 8 A (290 mA cm^{-2}) or higher, the non-uniformity in all the cells in the stack is more evident. The optimal operating current for a stack is in the range of 4–6 A

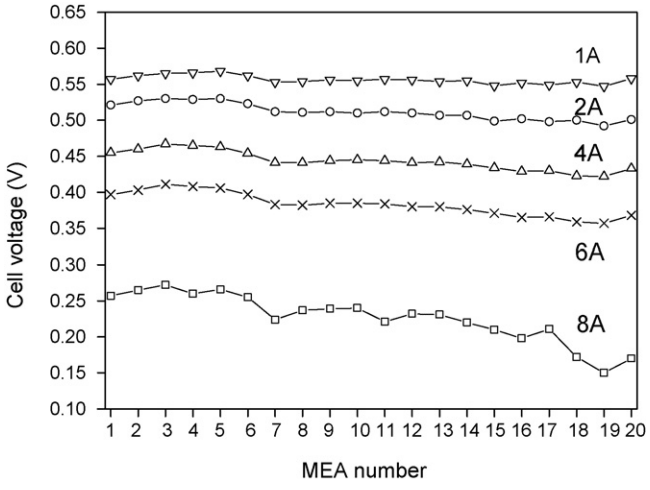

Fig. 6. Voltage distribution over individual cells in stack with Z-type flow at various currents at 50 °C; 1 M methanol flow rate 31.49 g min^{-1}; air flow rate 6 slm.

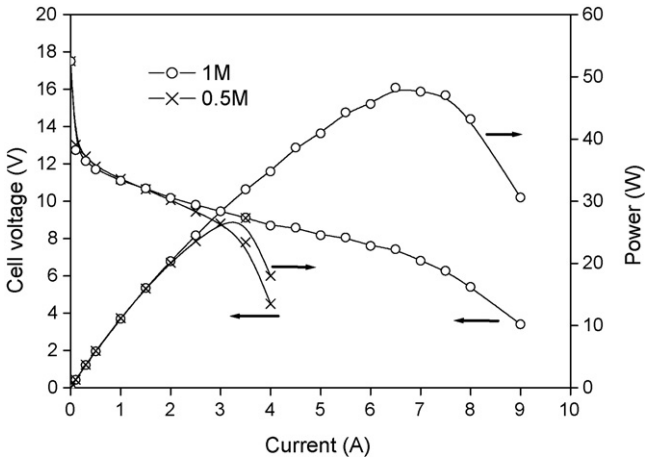

Fig. 7. Stack performance at different methanol concentrations at 50 °C; methanol flow rate 31.49 g min^{-1}; air flow rate 6 slm.

providing better stability, safety and power characteristics. It is considered that there is power loss due to the non-uniformity of flow and temperature distribution in stack resulting in the overall poor stack performance as shown in Figs. 5 and 6.

4.2. Effect of methanol concentration

Fig. 7 shows the performance of the stack with 1 and 0.5 M methanol solutions as fuel. At low current densities the power characteristics of the stack supplied with these two solutions are close. Performance with 0.5 M solution decreases sharply when current increases more than 3 A (100 mA cm^{-2}) due to the lack of methanol at the anode. Fig. 8 shows methanol crossover and water transfer in stack with different methanol concentrations at 50 °C. Methanol crossover in the stack with 1 M as fuel is evidently more than for 0.5 M due to greater swelling of the membrane at higher methanol concentration. As the current increases, methanol crossover decreases with the decrease in methanol concentration at the anode catalyst layer but water transfer increases due to increase in electro-osmosis. The methanol concentration is an important factor for water crossover. The water

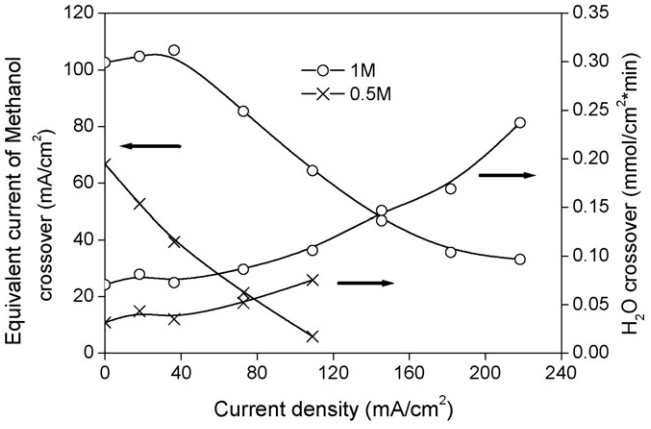

Fig. 8. Methanol crossover and water transfer in stack with different methanol concentrations at 50 °C; methanol solution flow rate 31.49 g min^{-1}; air flow rate 6 slm.

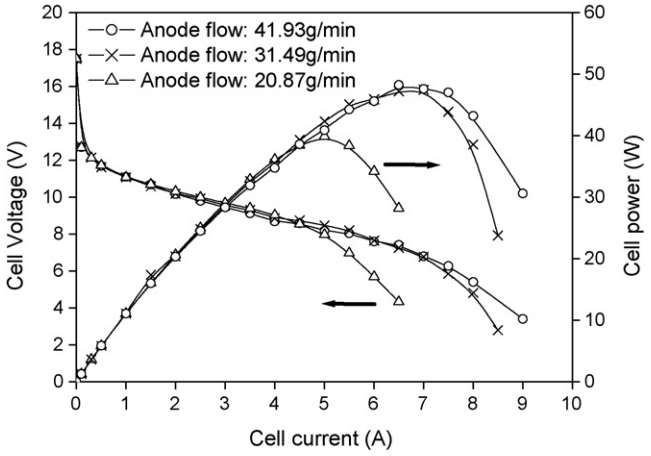

Fig. 9. Stack performances at 50 °C at various 1 M methanol flow rates; air flow rate 6 slm.

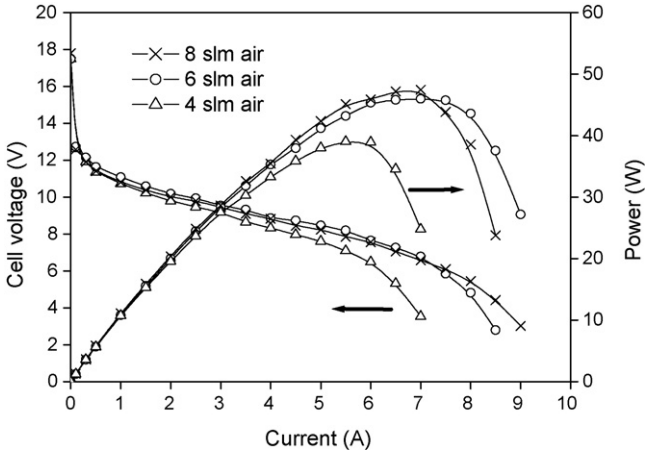

Fig. 11. Stack performances at 50 °C at various air flow rates; 1 M methanol flow rate 31.49 g min^{-1}.

crossover increases with an increase in methanol concentration. The higher methanol concentrations may cause membrane to swell resulting the pores to dilate allowing more water to pass through.

4.3. Effect of methanol flow rate

Three methanol flow rates of 20.87, 31.49 and 41.93 g min^{-1} are used to study the effect on stack power characteristics as shown in Fig. 9. The cell performance increases with methanol flow rate up to 31 g min^{-1} after which any further increase has no significant effect. Fig. 10 shows methanol crossover and water transfer for three different methanol flow rates. An increase in flow rate results in an increase in methanol crossover because the higher flow rate can maintain a higher methanol concentration over the entire channel of each cell. Moreover, methanol crossover across the membrane causes more water produced at the cathode. It brings about an increase in driving force of water from cathode to anode. At the same time, the increase in methanol crossover produces more water at cathode resulting in a decrease in water transfer.

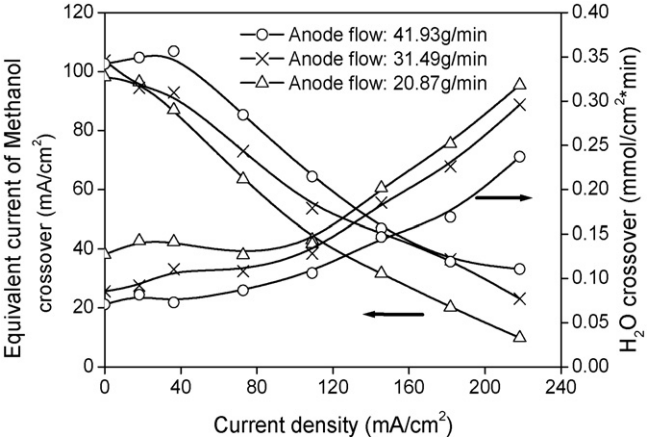

Fig. 10. Methanol crossover and water transfer in stack at 50 °C at various 1 M methanol flow rates; air flow rate 6 slm.

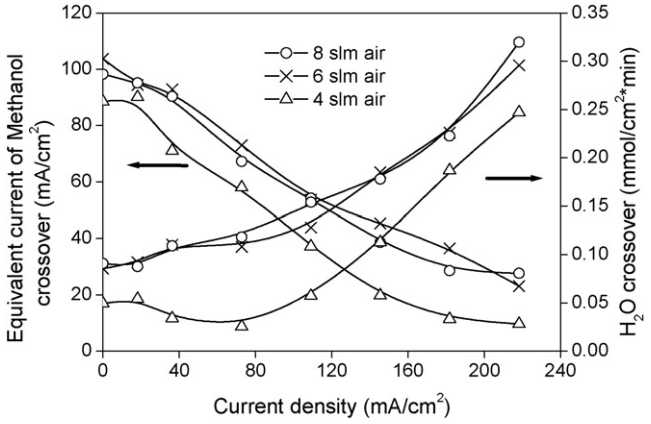

Fig. 12. Methanol crossover and water transfer in stack at 50 °C at various air flow rates; 1 M methanol flow rate 31.49 g min^{-1}.

4.4. Effect of air flow rate

Fig. 11 shows the effect of air flow rate on stack voltage and power output. The cell performance increases with air flow rate up to 6 slm, after which any further increase has no significant effect. The oxygen concentration decrease rapidly along the flow channel at lower air flow rate and at higher current densities. Air flow rates up to 6 slm can provide sufficient oxygen. Any further increase in flow rate hardly affects the stack performance.

The effect of air flow rates at the cathode on the methanol crossover and water transfer is shown in Fig. 12. The flux of both methanol and water through the membrane increases as the air flow rate increases. The effect is negligible when the air flow rate is greater than 6 slm. More air rate at the cathode means less water concentration which increases the driving force across the membrane; causing more water crossover.

5. Conclusions

The following conclusions can be drawn from this study:

1. The voltage distribution over cells in the stack is irregular due to non-uniformity in flow and temperature distribution. The

voltage distribution with Z-type flow is more uniform than with U-type flow. The non-uniformity is found to increase as current density increases.

2. The power characteristics of a stack with 1 M methanol solution as feed are better than with 0.5 M solution. The stack performance improves with the increase in methanol or air flow rates up to a point, after which an increase in these parameters has no significant effect.
3. Methanol crossover in the stack with 1 M methanol feed is more than 0.5 M due to the increase in swelling of the membrane at the higher solution concentration. An increase in methanol flow rate results in an increase in methanol crossover which in turn produces more water at cathode resulting in a decrease in water transfer. An increase in the air flow rate cause the removal of water produced at the cathode and thus an increase in the methanol and water flux through the membrane occurs. However, when the air flow rate increases more than 6 slm, no further increase is observed.
4. Under the optimal operating conditions, the rated current and power densities of the stack are 5 A (180 mA cm^{-2}) and 40 W (72.7 mW cm^{-2}), respectively at the operating temperature of 50 °C. Stoichiometric methanol flow rate and air flow rate are 3 (31.49 g min^{-1}) and 3.62 (6 slm), respectively, and the Faraday efficiency is 83.3%.

Acknowledgements

The work is funded by the National High Technology R&D Program of China (2003AA517070), the Key Grant International Cooperation Project of China (2004DFB02500) and Natural Science Foundation of China (50573041). Authors want to thank Mr. Daqiang Sun for his help during the experiments.

References

[1] A. Lokurlu, T. Grube, B. Höhlein, D. Stolten, Int. J. Hydrogen Energy 28 (2003) 703–711.
[2] R. Dillon, S. Srinivasan, A.S. Aricò, V. Antonucci, J. Power Sources 127 (2004) 112–126.
[3] M.A.J. Cropper, S. Geiger, D.M. Jollie, J. Power Sources 131 (2004) 57–61.
[4] A.S. Aricò, S. Srinivasan, V. Antonucci, Fuel Cells 1 (2001) 133–161.
[5] M.A. Hickner, H. Ghassemi, Y.S. Kim, B.R. Einsla, J.E. McGrath, Chem. Rev. 104 (2004) 4587–4612.
[6] M.P. Hogarth, T.R. Ralph, Platinum Metals Rev. 46 (2002) 146–164.
[7] E. Antolini, Mater. Chem. Phys. 78 (2003) 563–573.
[8] B. Gurau, E.S. Smotkin, J. Power Sources 112 (2002) 339–352.
[9] C.Y. Chen, J.Y. Shiu, Y.S. Lee, J. Power Sources 159 (2006) 1042–1047.
[10] H. Dohle, H. Schmitz, T. Bewer, J. Mergel, D. Stolten, J. Power Sources 106 (2002) 313–322.
[11] D. Buttin, M. Dupont, M. Straumann, R. Gille, J.C. Dubois, R. Orelas, G.P. Fleba, E. Ramunni, V. Antonucci, A.S. Aricò, P. Cretì, E. Modica, M. Pham-Thi, J.P. Ganne, J. Appl. Electrochem. 31 (2001) 275–279.
[12] A. Oedegaard, C. Hentschel, J. Power Sources 158 (2006) 177–187.
[13] D. Kim, J. Lee, T.H. Lim, I.H. Oh, H.Y. Ha, J. Power Sources 155 (2006) 203–212.
[14] R.Z. Jiang, C. Rong, D. Chu, J. Power Sources 126 (2004) 119–124.
[15] C. Xie, J. Bostaph, J. Pavio, J. Power Sources 136 (2004) 55–65.
[16] Y.J. Sohn, G.G. Park, T.H. Yang, Y.G. Yoon, W.Y. Lee, S.D. Yim, C.S. Kim, J. Power Sources 145 (2005) 604–609.
[17] Y. Liu, MS Thesis, Tsinghua University, Beijing, China, 2006.
[18] R.Z. Jiang, D. Chu, Electrochem. Solid-State Lett. 5 (2002) A156–A159.
[19] H. Dohle, J. Divisek, J. Mergel, H.F. Oetjen, C. Zingler, D. Stolten, J. Power Sources 105 (2002) 274–282.
[20] R.Z. Jiang, D. Chu, J. Electrochem. Soc. 151 (2004) A69–A76.
[21] V. Gogel, T. Frey, Y.S. Zhu, K.A. Friedrich, L. Jörissen, J. Garche, J. Power Sources 127 (2004) 172–180.
[22] J.A. Drake, W. Wilson, K. Killeen, J. Electrochem. Soc. 151 (2004) A413–A417.
[23] G. Vijayaraghavan, L. Gao, C. Korzeniewski, Langmuir 19 (2003) 2333–2337.